Inorg. Chem. **2005**, *44*, 2060–2066

Structure and Magnetism of a New Hydrogen-Bonded Layered Cobalt(II) Network, Constructed by the Unprecedented Carboxylate–Phosphinate Ligand $[O_2(C_6H_5)PCH_2CO_2]^{2-}$

Stefano Midollini,[†] Annabella Orlandini,*[,†] Patrick Rosa,[‡,§] and Lorenzo Sorace[§]

Istituto della Chimica dei Composti Organometallici, ICCOM, CNR, Via Madonna del Piano, 50019 Sesto Fiorentino, Firenze, Italy, Groupe de Sciences Moléculaires Institut de Chimie de la Matière Condensée de Bordeaux - CNRS UPR 9048 87, avenue du Docteur Schweitzer 33608 Pessac Cedex, France, and Dipartimento di Chimica and UdR INSTM Università di Firenze, Via della Lastruccia 3, 50019 Sesto Fiorentino Firenze, Italy

Received October 7, 2004

By hydrothermal reaction of $CoCl_2 \cdot 6H_2O$ with K_2pcc (H_2pcc = phenyl(carboxymethyl) phosphinic acid) at 423 K, a novel hybrid material of formula $[Co_2(pcc)_2(H_2O)_2] \cdot H_2O$ has been obtained. The compound, which is the first pcc/metal complex reported, exhibits a polymeric arrangement, where cobalt metal ions, linked together by bridging carboxylate and phosphinate oxygens, form infinite chains of edge-shared CoO_6 octahedra. The cobalt chains are in turn linked together through important hydrogen-bonding interactions, which create an infinite 2D architecture. The two crystallographically independent cobalt centers, both displaying distorted octahedral coordination, present different environments as one is surrounded by six ligand oxygens and the other by four ligand oxygens and by two water oxygens. Careful magnetic studies performed by a home-built alternating currnet susceptometer reveal that the system undergoes an antiferromagnetic transition below 2.0 K leading to a canted structure. Field-dependent studies further indicate the occurrence of a metamagnetic transition at a critical field of 650 ± 50 G.

Introduction

The synthesis of organic–inorganic hybrid materials is of great interest because these extended systems play a significant role for the investigation in the areas of catalysis, chirality, luminescence, magnetism, nonlinear optics, and porosity behavior.[1,2] Among these, metal phosphonates are very important for their structural tunability (being able to form networks extended in 1, 2, and 3 dimensions), for their chemical and thermal stability, and for their morphological similarity to well-studied phases such as LB films.[3] As a matter of fact, many examples have been reported where these compounds are stacked head to head and tail to tail to make layers of alternating polar (ions and oxygen atoms) and nonpolar (organic moieties) groups.[4–6]

Recently a variety of open-framework structures have been isolated by introducing different organic residues or connecting to the phosphonic acid other functional groups, such as carboxylate ligands.[7–15] On the other hand, relatively few examples of metal phosphinates[16,17] have been reported,

* Author to whom correspondence should be addressed. E-mail: annabella.bianchi@iccom.cnr.it.
[†] ICCOM, CNR.
[‡] Institut de Chimie de la Matière Condensée.
[§] Università di Firenze.

(1) Hagrman, P. J.; Hagrman, D.; Zubieta, J. *Angew. Chem., Int. Ed.* **1999**, *38*, 2639–2684.
(2) Allcock, H. R. *Adv. Mater*. **1994**, *6*, 106–115.
(3) (a) Cao, G.; Hong, H.-G.; Mallouk, T. E. *Acc. Chem. Res*. **1992**, *25*, 420–427. (b) Clearfield, A. *Curr. Opin. Solid State Mater. Sci.* **1996**, *1*, 268–278. (c) Clearfield, A. *Curr. Opin. Solid State Mater. Sci.* **2002**, *6*, 495–506 and references therein.
(4) Bakhmutova, E. V.; Ouyang, X.; Medvedev, D. G.; Clearfield, A. *Inorg. Chem.* **2003**, *42*, 7046–7051.
(5) Kong, D.; Li, Y.; Ross, J. H., Jr.; Clearfield, A. *Chem. Commun*. **2003**, 1720–1721.
(6) Burlholder, E.; Golub, V. O.; O'Connor, C. J.; Zubieta, J. *Inorg. Chim. Acta* **2002**, *340*, 127.
(7) Song, J.-L.; Zhao H.-H.; Mao, J.-G.; Dunbar, K. R. *Chem. Mater*. **2004**, in press.
(8) Mao, J.-G.; Clearfield, A. *Inorg. Chem*. **2002**, *41*, 2319–2324.
(9) Stock, N.; Frey, S. A.; Stucky, G. D.; Cheetham, A. K. *J. Chem. Soc., Dalton Trans*. **2000**, 4292–4296.
(10) Zhu, J.; Bu, X.; Feng, P.; Stucky, G. D. *J. Am. Chem. Soc*. **2000**, *122*, 11563–11564.
(11) Gutschke, S. O. H.; Price, D. J.; Powell, A. K.; Wood, P. T. *Angew. Chem., Int. Ed. Engl*. **1999**, *38*, 1088–1090.
(12) Distler, A.; Lohse, D. L.; Sevov, S. C. *J. Chem. Soc., Dalton Trans*. **1999**, 1805–1812.
(13) Ayyappan, S.; De Delgado, G. D.; Cheetham, A. K.; Ferey, G.; Rao, C. N. R. *J. Chem. Soc., Dalton Trans.* **1999**, 2905–2907.
(14) Distler, A.; Sevov, S. C. *Chem. Commun*. **1988**, 959–960.

10.1021/ic048602x CCC: $30.25
Published on Web 02/19/2005

Chart 1

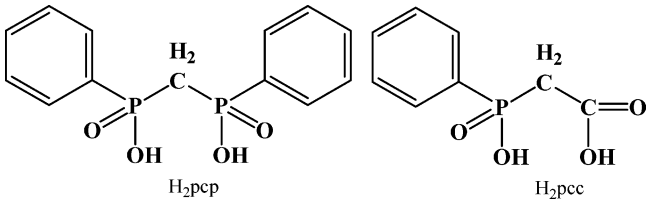

which generally present polymeric monodimensional structures. Recently we have found that the bifunctional anion of the P,P′-diphenylmethylene diphosphinic acid (H_2pcp) (Chart 1) is capable of bridging metal ions to give also bidimensional hybrid materials. As a matter of fact, the complexes of formula M(pcp) (M = Zn(II)[18] and Pb(II),[19] show polymeric arrangement (respectively, 2D and 1D) built up by strong covalent bonds. The related hydrated compounds $[M(pcp)(H_2O)_3]\cdot H_2O$ (M = Mn(II), Co(II), and Ni(II)), which represent an isomorphous series, are constituted by 2D hydrogen-bonded materials.[20] Actually the latter are formed by chains built up by an alternating array of metal centers and P,P′-diphenylmethylenediphosphinate ligands, which are in turn connected through strong hydrogen-bond links, to form corrugated 2D layers.

In the context of our investigation about the reactivity of the bifunctional phenyl(carboxymethyl)phosphinic acid (H_2-pcc) (Chart 1) toward metal ions, the compound $[Co_2(PhPO_2\text{-}CH_2CO_2)_2(H_2O)_2]\cdot H_2O$ **1** was obtained as single crystals by the hydrothermal reaction of $CoCl_2\cdot 6H_2O$, potassium phenyl-(carboxymethyl)phosphinate (K_2pcc), and deionized water.

Experimental Section

Materials and Methods. K_2pcc was prepared as previously reported.[21] The hydrothermal reaction was performed in a stainless steel autoclave with a Teflon insert (ca. 20 mL capacity) constructed in the Institute.

Preparation of $[Co_2(pcc)_2(H_2O)_2]\cdot H_2O$, 1. Hydrothermal reaction of $CoCl_2\cdot 6H_2O$ (51 mg, 0.21 mmol), K_2pcc (60 mg, 0.21 mmol), and 5 mL of deionized water in the ratio 1:1:1333 for 3 days at 423 K, followed by slow cooling at room temperature, produced pink-red needles of the complex in about 30% yield. The compound was filtered, washed with water, and dried in air at room temperature. Anal. Calcd for $C_{16}H_{20}Co_2O_{11}P_2$: C, 33.82; H, 3.55. Found: C, 33.10; H, 3.45.

Crystallography. Diffraction data for the cobalt derivatives were collected at room temperature on a Philips PW 1100 automatic diffractometer. Unit cell parameters were determined by least-squares refinement of the setting angles of 25 carefully centered reflections. Crystal data and data collection details are given in Table 1. The intensities I were assigned the standard deviations $\sigma(I)$ calculated by using a value of 0.03 for the instability factor k.[22] They were corrected for Lorentz polarization effects, and an empirical absorption correction was applied.[23] Atomic scattering factors for neutral atoms were taken from ref 24. Both $\Delta f'$ and $\Delta f''$ components of anomalous dispersion were included for all non-hydrogen atoms.[25] The structure was solved by direct methods and refined by full-matrix F^2 refinement, with anisotropic thermal parameters assigned to cobalt, phosphorus, and oxygen atoms. The hydrogen atoms were introduced in their calculated positions riding on their carbon atoms, with thermal parameters 10% larger than those of the respective carbon atoms. The function minimized during the refinement was $\Sigma w(F_0^2 - F_c^2)^2$, with $w = 1/[\sigma^2(F_0^2) + (0.0106P)^2 + 20.47P]$ ($P = (\max(F_0^2, 0) + 2F_c^2)/3$). All the calculations were performed on a Pentium processor using the package WINGX[26] (SIR97,[27] SHELX97,[28] ORTEP-III[29]).

Table 1. Crystal Data and Structure Refinement

formula	$C_{16}H_{20}Co_2O_{11}P_2$
fw	568.12
T, K	293(2)
λ, Å	1.54180
cryst syst, space group	monoclinic, $P2_1/c$
a, Å	23.185(9)
b, Å	9.202(1)
c, Å	9.706(4)
α, deg	90
β, deg	89.94(5)
γ, deg	90
V, Å^3	2070.8(12)
Z	4
ρ_{calcd}, g cm^{-3}	1.822
μ, mm^{-1}	14.556
F(000)	1152
cryst size, mm	0.40 × 0.075 × 0.037
θ range for data collection, deg	3.81−49.98
reflns collecd/indpnt	3541/2120
refinement method	full-matrix least-squares on F^2
data/restraints/parameters	2120/0/176
GOF on F^2	0.944
R1/wR2 [$I > 2\sigma(I)$][a]	0.0521/0.1077
R1/wR2 (all data)	0.0607/0.1126
largest diff. peak and hole, e.A^{-3}	0.390 and −0.328

[a] $R1 = \Sigma(||F_o| - |F_c||)/\Sigma|F_o|$; $wR2 = \{\Sigma[w(|F_o^2 - F_c^2|)^2/\Sigma[w(F_o^2)^2]\}^{1/2}$.

Magnetic Measurements. Temperature- (2−300 K) and field-dependent (0−6 T) magnetization of a microcrystalline powder sample of **1** have been investigated with a Cryogenic S600 SQUID magnetometer. The powder was pressed into a pellet to avoid preferential orientation of the microcrystallites. Data were corrected for the diamagnetism of the sample holder and measured in the same range of field and temperature and for the intrinsic diamagnetic contribution for the sample estimated through Pascal's constants.

(15) Drumel, S.; Janvier, P.; Barboux, P.; Bujoli-Doeff, M.; Bujoli B. *Inorg. Chem.* **1995**, *34*, 148−156.
(16) Grohol, D.; Ginge, F.; Clearfield, A. *Inorg. Chem.* **1999**, *38*, 751−756.
(17) Oliver, K. W.; Rettig, S. J.; Thomson, R. C.; Trotter, J.; Xuia, S. *Inorg. Chem.* **1997**, *36*, 2465−2468.
(18) Cecconi, F.; Dakternieks, D.; Duthie, A.; Ghilardi, C. A.; Gili, P.; Lorenzo-Luis, P. A.; Midollini, S.; Orlandini, A. *J. Solid State Chem.* **2004**, *177*, 786−792.
(19) Cecconi, F.; Ghilardi, C. A.; Midollini, S.; Orlandini, A. *Inorg. Chem. Commun.* **2003**, *6*, 546−548.
(20) Berti, E.; Cecconi, F.; Ghilardi, C. A.; Midollini, S.; Orlandini, A.; Pitzalis, E. *Inorg. Chem. Commun.* **2002**, *3*, 1041−1043.
(21) Cecconi, F.; Dominguez, S.; Masciocchi, N.; Midollini, S.; Sironi, A.; Vacca, A. *Inorg. Chem.* **2003**, *42*, 2350−2356.
(22) Corfield, P. W. R.; Doedens, R. J.; Ibers, J. A. *Inorg. Chem.* **1967**, *6*, 197−204.
(23) Parkin, S.; Moezzi, B.; Hope, H. *J. Appl. Crystallogr.* **1995**, *28*, 53−56.
(24) *International Tables for X-ray Crystallography*; Kluwer: Dordrecht, 1992; Vol. C, p 500.
(25) *International Tables for X-ray Crystallography*; Kluwer: Dordrecht, 1992; Vol. C, p 219.
(26) Farrugia, L. J. *J. Appl. Crystallogr.* **1999**, *32*, 837−838.
(27) Altomare, A.; Burla, M. C.; Camalli, M.; Cascarano, G. L.; Giacovazzo, C.; Guagliardi, A.; Moliterni, A. G. C.; Polidori, G.; Spagna, R. *J. Appl. Crystallogr.* **1999**, *32*, 115−119.
(28) Sheldrick, G. M. *SHELX97*; University of Göttingen: Göttingen, Germany, 1997.
(29) Burnett, M. N.; Johnson C. K. *ORTEP-III*; Oak Ridge National Laboratory: Oak Ridge, TN, 1996.

A home-built induction susceptometer employed for the alternating current (AC) measurements at low temperature (1.5−20 K) and low field (0−0.2 T) at variable oscillating frequency (90−9529 Hz) is herein described for future reference.[30] The probe consists of a first-order gradiometer, with 9-mm diameter counterwinded secondaries and an 11.4-mm diameter primary circuits, built with Cu wire over a chalk-Araldite body with a 6-mm bore. A Cernox thermometer was inserted between the secondaries for both control and sample temperature. After primary−secondaries coupling had been minimized, primary field homogeneity was calculated (FEMM 4.0 software)[31] at better than 0.2%. The probe was adapted within an Oxford cryostat with a 12-T magnet and a 1.4−300-K variable temperature insert. A SR830 Stanford Research Systems Lock-In was used as both an AC current source and a secondary signal analyzer. Tests and calibration with a paramagnetic $[Gd_2(SO_4)_3]\cdot 7H_2O$ pellet and a 5-mm superconducting Pb sphere[32] availed an optimum working range of 1.5−30 K and 20−10 000 Hz, with up to 1.3 G for the exciting AC field. The sample signal is extracted over both secondary positions with a stepper motor. This allows particularly to minimize the field contribution to the secondaries signals and to make measurements with fields up to a few Teslas.

Results and Discussion

Pink-red needles of **1** are obtained in moderate yield (30%) by hydrothermal reaction of cobalt chloride with K_2pcc at 423 K. Attempts to improve the yield of the reaction by varying in turn the molecular ratios and/or the temperature were unsuccessful. The crystals are practically insoluble in water, at room temperature. However the solid slowly dissolves in the mother water solution (ca. 3 days). Evaporation of the resulting pink solution does not allow the recovery of the title compound.

Description of the Structure. The structure of **1**, established by X-ray analysis, consists of hybrid carboxylate−phosphinate $[Co_2(pcc)_2(H_2O)_2]$ polymer and solvate water molecules. The asymmetric unit consists of two cobalt atoms, two pcc^{2-} ligands, and two coordinated and one crystallization water molecules. The cobalt metals, which are linked together through bridging carboxylate and phosphinate oxygens, create an infinite chain of edge-shared CoO_6 octahedra, which propagates in zigzag down the *z* axis (Figures 1 and 2). Both the independent cobalt atoms display distorted octahedral geometries, even if the distortion is significantly larger in one of them, as the trans angles range 170.9(2)−177.8(2)° and 161.2(2)−169.4(2)° for Co1 and Co2, respectively. The two cobalt centers present different environments, as a matter of fact, while the Co1 is linked to six oxygen atoms from four different pcc ligands (Co−O range 2.037−2.115(4) Å), the Co2 is surrounded by four oxygens from four different pcc ligands and by two coordinated water molecules (Co−O range 2.058(5)−2.195(5) Å) (see Table 2).

Actually the acidic oxygens of both functional groups are deprotonated, and each pcc ligand, acting as tridentate, uses the phosphinate oxygens and one carboxylate oxygen to chelate and coordinate four metal atoms (stable six-membered rings O−P−C−C−O−Co and O−P−O−Co−O−Co being formed). The remaining free carboxylate oxygen atoms in both pcc ligands play an important role, as they are involved in an extended network of hydrogen bonds with the coordinated and solvated water molecules. Through such hydrogen interactions the cobalt ribbons are in turn linked together, creating an infinite 2D architecture, extended in the *yz* plane (Figure 3). The more important hydrogen bondings (<3.0 Å) relative to the free carboxylate oxygens are (Å): O4···O9^{I} 2.78 ($I = x, 1 + y, z$), O4···O9^{II} 2.96 (II $= x, 0.5 - y, 0.5 + z$), O4···O11 2.72, and O8···O10^{I} 2.75. Another significant hydrogen interaction, which involves a phosphinate oxygen bonded to the metal and the solvent water molecule, is: O2···O11^{III} 2.81 (III $= x, 1.5 - y, -0.5 + z$).

Interestingly, the values of the P−O bond lengths are well in agreement with the nature of the P−O bond, as the larger ones (P1−O1 1.535(5) and P2−O6 1.548(5) Å) are involved in two-metal bridging and the shorter ones (P1−O2 1.508(5) and P2−O5 1.508(4)) Å in one-metal bonds. In concern for the C−O bond distances, the larger standard deviations as well as the presence of several hydrogen bonds make a similar rationalization more difficult.

The 2D layers made up by the inorganic moieties are shielded from one another by the organic part of the pcc

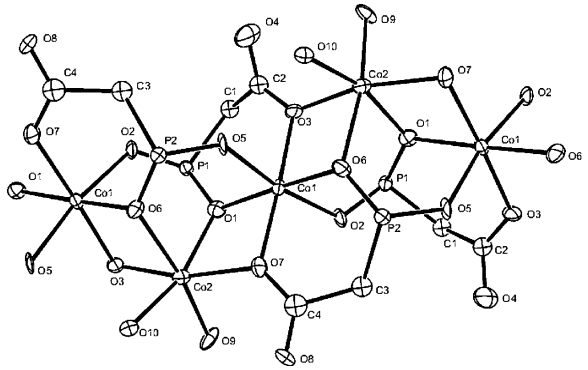

Figure 1. Portion of the polymer showing the complete connectivity to Co1 and Co2 metals. Phenyl rings omitted for sake of clarity.

Table 2. Selected Bond Lengths (Å) and Angles (deg)[a]

Co(1)−O(3)	2.037(5)	Co(2)−O(6)	2.177(5)
Co(1)−O(6)#1	2.053(5)	Co(2)−O(1)	2.195(5)
Co(1)−O(7)#1	2.069(5)	P(1)−O(2)	1.508(5)
Co(1)−O(5)	2.101(4)	P(1)−O(1)	1.535(5)
Co(1)−O(1)	2.101(5)	P(2)−O(5)	1.508(4)
Co(1)−O(2)#1	2.115(4)	P(2)−O(6)	1.548(5)
Co(1)−Co(2)	3.148(2)	O(3)−C(2)	1.212(9)
Co(2)−O(9)	2.058(5)	O(4)−C(2)	1.245(10)
Co(2)−O(7)#1	2.062(5)	O(7)−C(4)	1.293(9)
Co(2)−O(10)	2.064(5)	O(8)−C(4)	1.223(10)
Co(2)−O(3)#2	2.135(5)		
O(3)−Co(1)−O(6)#1	86.4(2)	O(3)#2−Co(2)−O(6)	81.0(2)
O(3)−Co(1)−O(7)#1	177.8(2)	O(7)#1−Co(2)−O(1)	79.4(2)
O(6)#1−Co(1)−O(1)	176.7(2)	O(10)−Co(2)−O(1)	164.7(2)
O(7)#1−Co(1)−O(1)	81.4(2)	Co(1)−O(1)−Co(2)	94.2(2)
O(5)−Co(1)−O(2)#1	170.9(2)	Co(1)−O(3)−Co(2)#1	97.1(2)
O(7)#1−Co(2)−O(3)#2	161.2(2)	Co(1)#2−O(6)−Co(2)	95.3(2)
O(9)−Co(2)−O(6)	169.4(2)	Co(2)#2−O(7)−Co(1)#2	99.3(2)

[a] Symmetry transformations used to generate equivalent atoms: #1, $x, -y + 1/2, z + 1/2$; #2, $x, -y + 1/2; z - 1/2$.

(30) Nikolo, M. *Am. J. Phys.* **1995**, *63*, 57−65.
(31) See: http://femm.foster-miller.com/.
(32) Goldfarb, R. B.; Minervini, J. V. *Rev. Sci. Instrum.* **1984**, *55*, 761−64.

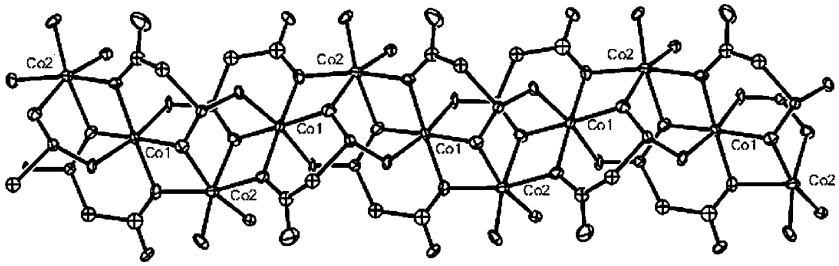

Figure 2. Propagation of the ribbons along the *z* axis.

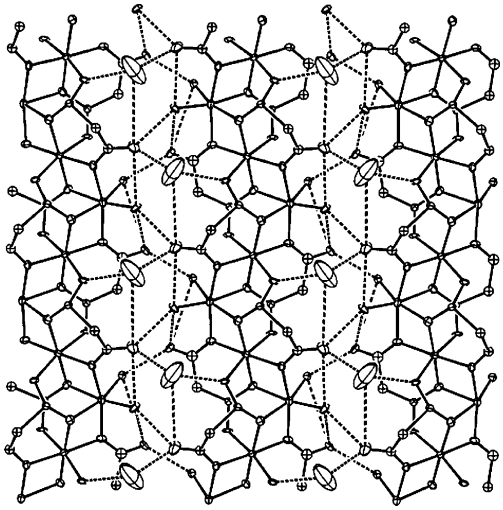

Figure 3. Portion of the polymer showing the layer constructed through hydrogen-bonding interactions. Propagation of the layer in the *yz* plane.

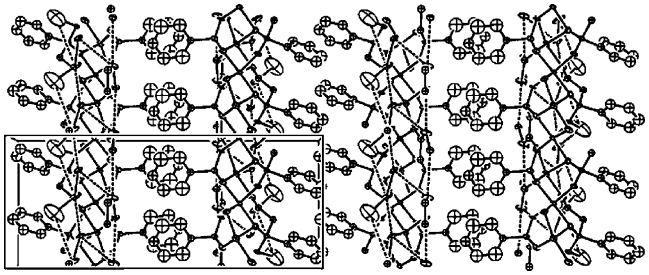

Figure 4. Complete packing diagram. View normal to [010].

ligand, namely, the phenyl rings, which present a relative disposition with the minimum distance between ring centroids of 4.76 Å. The complete packing with a view normal to [010] is reported in Figure 4.

In agreement with the presence of the hydrogen bonding network, the IR spectrum shows two quite broad bands centered at ca. 3250 and 1580 cm^{-1}, attributable, respectively, to the stretching and the bending vibration of H_2O.

It is noteworthy that the title compound is the first metal complex reported with the mixed bifunctional carboxylate-phosphinate ligand pcc^{2-}. Only the structure of a methoxy[33] or an ethoxy[34] derivative of the H_2pcc acid has been reported, as far as we know. With related dihydrogenphosphonoacetate ($PO_3HCH_2COOH^-$) and phosphonomethyl acetate (PO_3CH_2-

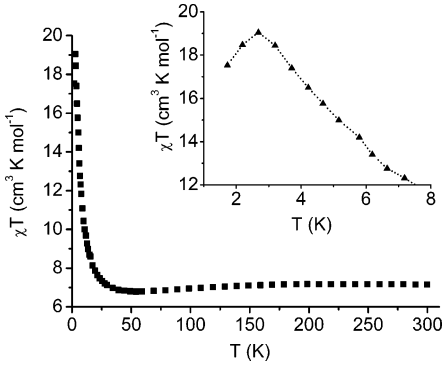

Figure 5. χT vs T plot of complex **1**. The inset shows the detail of the low-temperature part, evidencing the maximum in χT reached at 2 K.

$CH_2CO_2^{3-}$) ligands, few structures containing Ca(II),[35] Mg(II),[35] Co(II),[14,35] Mn(II),[9] Zn(II),[15] Sn(II),[36] or Pb(II)[13] have been described.

Magnetic Properties. The χT vs T plot of complex **1** (Figure 5) evidences a room-temperature value of 7.2 cm^3 K mol^{-1}, which falls within the reported range for similar polymeric phosphonato complexes.[37−39] Upon lowering the temperature, three different regions are clearly observed:

(i) Down to 55 K, a slow decrease of the χT value down to 6.8 cm^3 K mol^{-1} is observed. This behavior is probably due to the depopulation of the excited levels arising from the splitting of the $^4T_{2g}$ ground state for Co(II) ions following the combined action of low symmetry crystal field effects and spin−orbit coupling.[40]

(ii) Below 55 K, a net increase in χT is observed, to reach 19.1 cm^3 K mol^{-1} at 2.7 K, strongly indicating the existence of sizable magnetic coupling interaction within the chains. The minimum in χT observed at 55 K can arise as a consequence of antiferromagnetic interactions between the two crystallographically different cobalt centers.[41] Indeed, in the low-temperature region, these can be assumed to have

(33) (a) Galdecki, Z.; Glowka, M. L. *Acta Crystallogr., Sect. B* **1977**, *33*, 2650. (b) Galdecki, Z.; Glowka, M. L. *Acta Crystallogr., Sect. B* **1978**, *34*, 2938.
(34) Kielbasinski, P.; Goralczyk, P.; Mikolajczyk, M.; Wieczorek, M. W.; Majzner, W. R. *Tetrahedron: Asymmetry* **1998**, *9*, 2641−2650.
(35) Slepokura, K.; Piatkowska, A.; Lis, T. *Z. Kristallogr.* **2002**, *217*, 614−621.
(36) Adair, B. A.; Neeray, S.; Cheetham, A. K. *Chem. Mater.* **2003**, *15*, 1518−1529.
(37) Zheng, L. M.; Gao, S.; Yin, P.; Xin, X.-Q. *Inorg. Chem.* **2004**, *43*, 2151−2156.
(38) Lloret, F.; De Munno, G.; Julve, M.; Cano, J.; Ruiz, R.; Caneschi, A. *Angew. Chem., Int. Ed. Engl.* **1998**, *37*, 135−138.
(39) Kurmoo, M.; Kumagai, H.; Green, M. A.; Lovett, B. W.; Blundell, S. J.; Ardavan, A.; Singleton, J. *J. Solid State Chem.* **2001**, *159*, 343−351.
(40) Griffith, J. S. *The Theory of Transition Metal Ions*; Cambridge University Press: Cambridge, 1961.
(41) Caneschi, A.; Gatteschi, D.; Lalioti, N. V.; Sangregorio, C.; Sessoli, R.; Venturi, G.; Vindigni, A.; Rettori, A.; Pini, M. G.; Novak, M. A. *Angew. Chem., Int. Ed.* **2001**, *40*, 1760−1763.

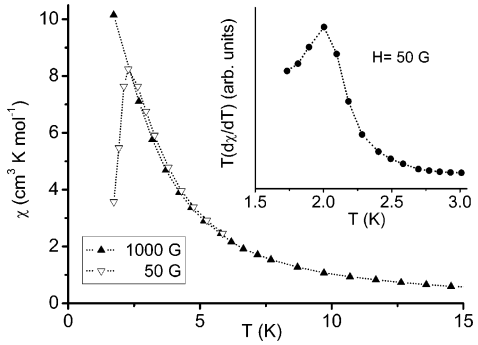

Figure 6. Plot of χ vs T behavior for **1** at 50 and 1000 G, evidencing the suppression of the antiferromagnetic transition at the latter field. The inset shows the determination of the actual transition temperature through the evaluation of the maximum of $Td\chi/dT$.

an effective spin $S = {}^1/_2$[40] with largely anisotropic g values differing from one center to another and antiferromagnetic interactions between them can then lead to a ferrimagnetic-like structure. The observed minimum can also arise as a consequence of the competing effects of ligand field effects and ferromagnetic interaction between Co centers. It has however to be pointed out that due to the peculiar electronic structure of octahedral Co(II) the anisotropic interactions are supposedly of comparable intensity, and even larger, than isotropic ones. As a consequence, ferro- (antiferro)magnetic coupling does not necessarily yield parallel (antiparallel) alignments of the spins but a more complex magnetic structure (see infra). Because of this complexity, it is then not possible to fit the magnetic data using a reliable model. Anyhow, the observation of a substantial increase in χT only below 50 K points to fairly moderate intrachain interactions, of the order of 30 cm^{-1}. This can be understood if one considers that the Co−O−Co angles between edge-sharing octahedra, even if somewhat tilted, are all smaller than 100°. In this region, the interaction passes from antiferromagnetic to ferromagnetic and it is then expected to be quite small, whatever its nature.[39,42]

(iii) The third region is finally observed down to 2 K, where χT decreases to 17.5 cm^3 K mol^{-1}, suggesting the existence of additional weak antiferromagnetic interactions (Figure 5 inset).

The comparison of χ (note that here the quantity actually measured is the ratio between the magnetization and the applied magnetic field) vs T curves at 50 and 1000 G applied fields (Figure 6) gives additional information. At the lower field, a clear sign of a transition to an antiferromagnetic state is observed with a maximum at 2.3 K. The critical temperature, taken as the maximum of the $Td\chi/dT$ vs T curve (Figure 6 inset), was estimated to occur at 2.0 K.[43] On the other hand, no maximum is observed at 1000 G, thus indicating that the transition is suppressed at this field. Interestingly, ZFC/FC curves measured at 50 G (not shown) did not evidence any divergence, thus indicating that no hysteretic phenomenon is active below the ordering temperature.

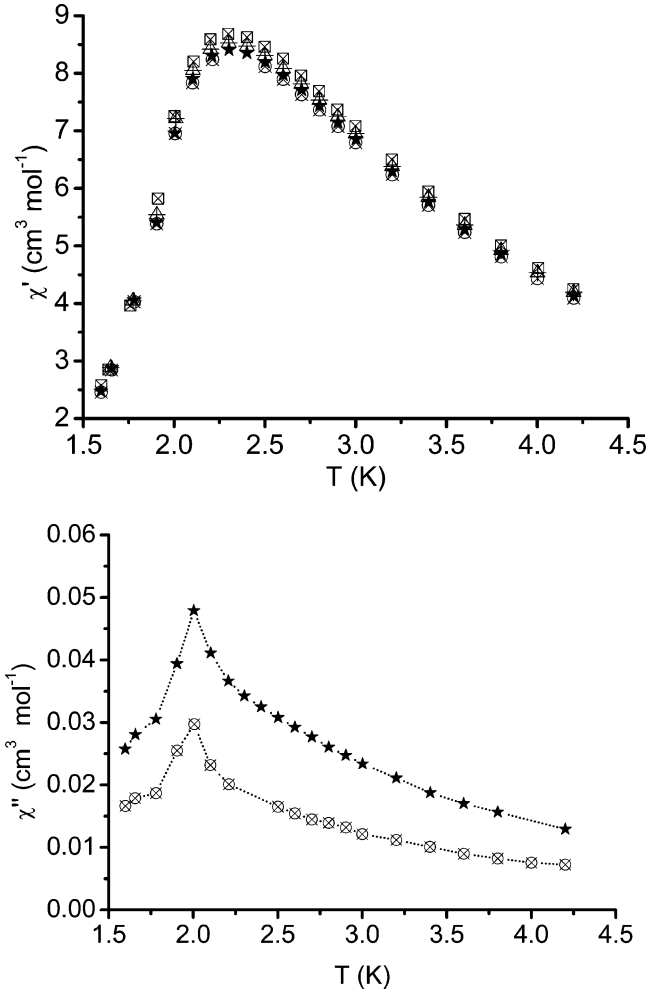

Figure 7. AC susceptibility of **1** in zero DC field as a function of temperature measured at different frequencies. (Crossed squares, 90 Hz; crossed triangles, 664 Hz; crossed circles, 4895 Hz; stars, 9529 Hz.) (a) In-phase contribution, (b) out-of-phase contribution (only the 2 highest frequencies are shown, the lowest ones not showing any peak; see text for details).

The analysis of the magnetic properties of this system through AC susceptibility measurements as a function of frequency and temperature helped substantially in clarifying the magnetic behavior of **1** at low temperature. The appearance of a well-defined maximum in χ' vs T measurements at $T = 2.3$ K (Figure 7a), whose position is independent of frequency, confirms the transition to a long-range ordered state. Interestingly, a very small signal showing its maximum at 2.0 K, independent of frequency, is observed in χ'' (Figure 7b).

This is a signature of the presence of a slow relaxing component and might suggest the occurrence of a weak ferromagnetic contribution resulting from a canted antiferromagnetic structure. In this framework, the absence of an intermediate antiferromagnetic phase between the paramagnetic and the weak ferromagnetic one may be indicative of the predominant influence of the single ion anisotropy over the exchange coupling interaction.[11] While at first sight the

(42) (a) Goodenough, J. B. *Magnetism and the Chemical Bond*; Wiley: New York, 1963. (b) Goodenough, J. B. *Phys. Rev.* **1955**, *100*, 564. (c) Kanamori, J. *J. Phys. Chem. Solids* **1959**, *10*, 87.
(43) Fisher M. E. *Proc. R. Soc. (London)* **1960**, *A 254*, 66.

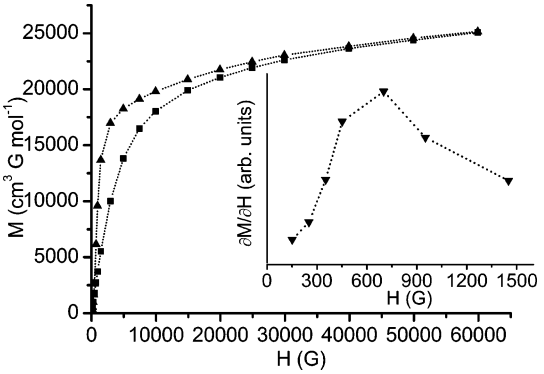

Figure 8. M vs H curve of **1** measured at 1.8 (▲) and 4.2 K (■). The inset shows the low-field derivative of the curve measured at 1.8 K, as to evidence the occurrence of a metamagnetic transition at around 0.07 T.

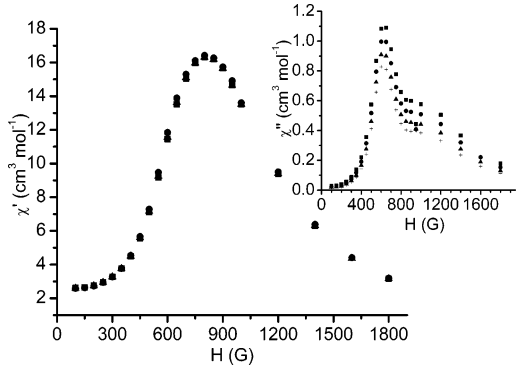

Figure 9. In-phase contribution to AC susceptibility of **1** as a function of field measured at 1.6 K and different frequencies. The inset shows the out-of-phase contribution. (●, 4111 Hz; +, 5440 Hz; ▲, 7200 Hz; ■, 9529 Hz.)

observation of a contribution to the out of phase susceptibility might appear as contradicting the nonobservation of a ZFC/FC divergence, it has to be considered however that χ'' is indeed of very small magnitude (at its maximum, it is only about 1% of χ'), and it is only visible at the highest frequencies, thus being completely compatible with the direct current (DC) measurements.

An alternative explanation for the appearance of a maximum in χ'', which does not require invoking a canted structure in the antiferromagnetic state, could in principle be the onset of slow relaxation of the single chains magnetization (Glauber dynamics),[41] which is then suppressed below the transition to the antiferromagnetic state.

Field-dependent magnetization (Figure 8) curves were recorded above and below the transition temperature (1.8 and 4.2 K, respectively). At the lower temperature, the occurrence of a metamagnetic transition around 700 G is clearly evident as a maximum in $\partial M/\partial H$ vs H curve (inset of Figure 8). At both temperatures, the value of saturation for the magnetization is in good agreement with what is expected for two Co(II) ions ($g_{ave} = 4.3$, $S_{eff} = {}^1/_2$), indicating that the antiferromagnetic interaction leading to the transition has been completely overcome as is expected for a metamagnetic transition. It has finally to be mentioned here that due to the partial overlapping with the low-field tail of the metamagnetic transition it has not been possible to measure the saturation value of the weak ferromagnetic component and thus to assess the canting angle of the spins.

To obtain a more accurate estimate of the metamagnetic transition field, AC susceptibility measurements (Figure 9) as a function of the field were performed, clearly showing that the metamagnetic transition occurs at $H = 650 \pm 50$ G (taken as the maximum in χ''). Interestingly, AC measurements also showed that at fields lower than that inducing the transition, both χ' and χ'' are independent of frequency. In agreement with this observation no hysteresis has been observed in the M vs H curve in DC measurements. On the other hand, some frequency dependence in χ'' is observed above the metamagnetic transition (around 1200 G). This suggests that once the paramagnetic phase has been restored by application of a field, magnetization relaxation times of the order of magnitude of the applied frequency, which are much probably connected with the 1D nature of the Co chains, characterize the system.[40]

The observation of canted magnetic structure is quite common for Co(II)-containing complexes,[11,37−39,44−46] and it has been previously reported for several metal−phosphonates-based systems.[47] In the present case, it indicates that, while far apart from each other, the 1D chains interact strongly enough within the 2D sheets which on their turn are interacting between each other to yield a long-range 3D magnetic ordered state. This is not completely surprising as antiferromagnetic long-range order in layered systems has been observed in the past for compounds with interlayer distance as large as 14 Å.[39]

On this respect, it has to be noted that in **1** the in-layer interchain interaction can be transmitted both through the hydrogen-bonds network which constitute the architecture of the 2D sheets and through space (the shortest Co−Co interchain contacts being 7.442 and 7.836 Å). On the other hand, interlayer interaction could be in principle transmitted through π-stacking interactions between phenyl rings of pcc ligands. However, this exchange coupling path would involve the transmission of the interaction through the O−P−phenyl skeleton of the ligands, and it seems then reasonable to assume that it cannot be effective in transmitting the interlayer interaction. The other possible explanation is the occurrence of a dipolar-driven long-range ordering. It has

(44) Rabu, P.; Drillon, M.; Awaga, K.; Fujita, W.; Sekine, T. In *Magnetism: Molecules to Materials*; Miller, J. S., Drillon, M., Eds; Wiley-VCH: Weinheim-New York, 2001, pp 357−395, Vol. II.
(45) Losee, D. B.; McElearney, J. N.; Shankle, G. E.; Carlin, R. L.; Cresswell P. J.; Robinson T. W. *Phys. Rev. B* **1973**, *8*, 2185−2199.
(46) (a) Tian, Y. Q.; Cai, C. X.; Ren, X. M.; Duan, C. Y.; Xu, Y.; Gao, S.; You, X. Z. *Chem.−Eur. J.* **2003**, *9*, 5673−5685. (b) Kumagai, H.; Kepert, C. J.; Kurmoo, M. *Inorg. Chem.* **2002**, *41*, 3410−3422. (c) Cave, D.; Gascon, J. M.; Bond, A. D.; Teat S. J.; Wood, P. T. *Chem. Commun.* **2002** 1050−1051. (d) Masciocchi, N.; Galli, S.; Sironi, A.; Barea, E.; Navarro, J. A. R.; Salas, J. M.; Tabares, L. C. *Chem. Mater.* **2003**, *15*, 2153−2160.
(47) (a) Day, P. *J. Chem. Soc., Dalton Trans*. **1997**, 701−705; (b) Bellitto, C.; Federici F. *Inorg. Chem.* **2002**, *41*, 709−714. (c) Bellitto, C.; Federici, F.; Ibrahim, S. A. *Chem. Commun.* **1996**, 759−760. (d) Zheng, L. M.; Gao, S.; Song, H. H.; Decurtins, S.; Jacobson, A. J.; Xin, X. Q. *Chem. Mater.* **2002**, *14*, 3143−3147. (e) Altomare, A.; Bellitto, C.; Ibrahim, S. A.; Mohammed, M. R.; Rizzi, R. *J. Chem. Soc., Dalton Trans.* **2000**, 3913−3919. (f) Bellitto, C.; Bauer, E. M.; Ibrahim, S. A.; Mahmoud M. R.; Righini, G. *Chem.−Eur. J.* **2003**, *9*, 1324−1331. (g) Bellitto, C.; Federici, F.; Ibrahim, S. A. *Chem. Mater.* **1998**, *10*, 1076−1082.

indeed been shown that in layered systems the dipolar interlayer interactions are effective in leading to an ordered state, due to the divergence of the in-layer spin correlation length on lowering temperature. If the anisotropy axis of the single ion is pointing normal to the layer plane, dipolar interactions lead to a ferromagnetic configuration, while an antiferromagnetic transition is expected if single ion anisotropy forces the spin to lie in the layer plane.[44] In this framework, the shortest interlayer dipolar contacts, which measure 11.29 and 12.02 Å, should be considered as the driving force leading to the canted antiferromagnetic state. It has to be noted that as these interactions involve either the two crystallographically different Co(II) ions or noncentrosymmetric pairs, the proposed mechanism fulfills the symmetry requirements for the observation of a canted magnetic structure.[48] As far as the metamagnetic transition is concerned, it should be remembered that such a transition occurs in antiferromagnetic systems with large anisotropy when the applied field is high enough to overcome the overall 3D order and aligns the spin along the field without passing through a spin−flop phase. Given that it is necessary for a metamagnetic transition to occur and that the anisotropy field is larger than the exchange one, its detection confirms our supposition about the relative importance of anisotropic and exchange interaction in this system.[49]

Summary

The hydrothermal method has been exploited to prepare the first metal complex with the bifunctional carboxylate−phosphinate pcc ligand. It is an inorganic−organic hybrid polymer, where the structure is built up by infinite ribbons of edge-shared CoO_6 octahedra, which in turn are linked together through strong hydrogen-bonding interactions, to create a 2D architecture. The 2D layers, made up by the metal ions and the inorganic functionalities, are shielded from one another by the organic part of the ligand, namely, the phenyls. The analysis of the magnetic properties evidenced the existence of a largely anisotropic magnetic interaction propagating along the cobalt chains, which leads to a dominating 1D character; however, below 2 K a long-range 3D magnetic order occurs, notwithstanding the large distance between the single chains inside the 2D layers and between these.

Acknowledgment. S.M. gratefully acknowledges Mr. A. Traversi and Mr. C. Bartoli (ICCOM, Firenze) for the construction of the reactor for hydrothermal reactions and Dr. S. Costantini (Università di Firenze) for microanalyses. L.S. thanks Prof. R. Sessoli and A. Vindigni (Università di Firenze) for fruitful suggestions and the financial support of FIRB project of MIUR. P.R. gratefully acknowledges the financial support of German DFG (SPP 1137- Molekularer Magnetismus) and mainly the help, advice, and guidance of Prof. Miguel Novak and Dr. Walter Folly of Universidade Federal do Rio de Janeiro, Brazil, for the building and setup of the AC probe.

Supporting Information Available: X-ray crystallographic data in CIF format; perspective view of the asymmetric unit of complex **1**; tables of atomic coordinates, isotropic displacement parameters, and bond lengths and angles. This material is available free of charge via the Internet at http://pubs.acs.org.

IC048602X

(48) (a) Dzyaloshinskii, I. *J. Phys. Chem. Solids* **1958**, *4*, 241. (b) Moriya, T. *Phys. Rev.* **1960**, *120*, 91.

(49) Carlin, R. L.; Van Duyneveldt, A. J. *Magnetic Properties of Transition Metal Compounds*; Springer-Verlag: New York-Heidelberg-Berlin, 1977.